Monthly Notices
of the
ROYAL ASTRONOMICAL SOCIETY

MNRAS **435,** 992–998 (2013)
Advance Access publication 2013 August 28

doi:10.1093/mnras/stt1302

Monte Carlo simulation of ELT-scale multi-object adaptive optics deformable mirror requirements and tolerances

A. G. Basden,⋆ N. A. Bharmal, R. M. Myers, S. L. Morris and T. J. Morris

Department of Physics, South Road, Durham DH1 3LE, UK

Accepted 2013 July 14. Received 2013 July 2; in original form 2013 May 7

ABSTRACT

Multi-object adaptive optics (MOAO) has been demonstrated by the CANARY instrument on the William Herschel Telescope. However, for proposed MOAO systems on the next-generation extremely large telescopes (ELTs), such as ELT Adaptive optics for GaLaxy Evolution (EAGLE), many challenges remain. Here we investigate requirements that MOAO operation places on deformable mirrors (DMs) using a full end-to-end Monte Carlo adaptive optics (AO) simulation code. By taking into consideration a prior global ground-layer (GL) correction, we show that actuator density for the MOAO DMs can be reduced with little performance loss. We note that this reduction is only possible with the addition of a GL DM, whose order is greater than or equal to that of the original MOAO mirrors. The addition of a GL DM of lesser order does not affect system performance (if tip/tilt star sharpening is ignored). We also quantify the maximum mechanical DM stroke requirements (3.5 μm desired) and provide tolerances for the DM alignment accuracy, both lateral (to within an eighth of a sub-aperture) and rotational (to within 0.2). By presenting results over a range of laser guide star asterism diameters, we ensure that these results are equally applicable for laser tomographic AO systems. We provide the opportunity for significant cost savings to be made in the implementation of MOAO systems, resulting from the lower requirement for DM actuator density.

Key words: instrumentation: adaptive optics – instrumentation: high angular resolution – methods: numerical – techniques: image processing.

1 INTRODUCTION

The proposed next-generation optical ground-based extremely large telescopes (ELTs), with primary mirror diameters of over 30 m, are currently in the design phase. These facilities, which will depend on adaptive optics (AO; Babcock 1953) for their operation, will provide astronomers with the necessary resolutions and light collecting areas to probe the universe with unprecedented sensitivity. The 39 m European Extremely Large Telescope (E-ELT) has a suite of planned instruments, one of which, the proposed ELT Adaptive optics for GaLaxy Evolution (EAGLE) instrument (Cuby et al. 2008), uses multi-object adaptive optics (MOAO; Gendron et al. 2011) to deliver a high degree of AO correction over a wide field of view. MOAO systems operate in open loop, i.e. the wavefront sensors (WFSs) do not sense the changes applied to the deformable mirrors (DMs). The EAGLE instrument will operate with six laser guide stars (LGSs) and up to five natural guide stars (NGSs; Rousset et al. 2010), delivering correction for up to 20 separate science fields each 1.65 arcsec in diameter, spread across a 10 arcmin field of view (with the central 5 arcmin being well corrected), with a 7.3 arcmin technical field.

The design of any AO system requires extensive numerical simulation and modelling of AO performance so that key design parameters can be determined, and to ensure that the science goals will be achievable. The Durham AO simulation platform (DASP; Basden et al. 2007) is a Monte Carlo time-domain code that has been developed specifically for ELT simulation, including optional hardware acceleration (Basden et al. 2005; Basden 2007). It is an end-to-end parallelized code including detailed models of telescope and AO systems, allowing high-fidelity models to be produced.

The ELT designs include a large DM (M4, with 85 × 85 actuators for the E-ELT) early in the telescope's optical train (Nelson & Sanders 2008; Spyromilio et al. 2008), optically conjugated close to the ground level. Although the MOAO instruments typically operate in open loop (with the DMs placed after the WFS light has been picked off), this telescope DM is visible to the WFSs and therefore is operated in closed loop, with the WFSs being sensitive to changes in the DM surface. Although theoretically not required for an MOAO instrument (which has its own DMs, one for each corrected line of sight), this DM can be used to perform a global, ground-layer AO (GLAO) correction across the telescope

⋆ E-mail: a.g.basden@durham.ac.uk

field of view. Previous Monte Carlo-based numerical studies for EAGLE (Fusco et al. 2008; Basden, Myers & Butterley 2010a) have generally ignored this DM, rather assuming an idealized open-loop DM for each science field.

In this paper, we investigate some of the benefits that are available to an MOAO instrument by making use of this GLAO correction, with considerations given to the reductions in the required MOAO DM mechanical stroke capability and also the order of the MOAO DMs (i.e. the actuator count). We also consider the impact of DM misalignment on the performance of this MOAO system, thus providing information about acceptable alignment tolerances. Comparisons of our simulation results with other codes, both Monte Carlo and analytic, are also made.

In Section 2, we introduce the simulations including parameters that were used, and the investigations carried out. In Section 3, we present results and discuss their implications, and in Section 4 we draw our conclusions.

2 MOAO SIMULATION DETAILS

For the purposes of this paper, we have developed a model of an MOAO instrument using DASP. We assume a 42 m diameter telescope with a central obscuration of 6 m, ignoring effects due to the secondary support structure. We have settled on using older parameters for telescope diameter rather than the current 39 m diameter, so that these simulation results can easily be compared with previous simulations performed before downsizing of the E-ELT. The atmosphere is modelled using a nine-layer profile as given in Table 1, with a 30 m outer scale and a Fried's parameter (r_0) of 13.5 cm at 500 nm corresponding to seeing of 0.8 arcsec. This atmospheric profile has been chosen to match that used in many simulations performed at the European Southern Observatory (ESO; Le Louarn et al. 2012). Phase screens are sampled with a 3.125 cm spacing. The simulation consists of six LGSs arranged in a regular hexagon with each WFS being a Shack–Hartmann sensor with 84 × 84 sub-apertures (each 0.5 m in the pupil plane), each having 16 × 16 detector pixels. For simplicity, and so as not to confuse results unnecessarily, we assume that the tip-tilt signal from the LGSs is valid or, equivalently, that NGS tip-tilt correction is performed perfectly. This allows us to focus on tomographic wavefront reconstruction from the LGSs, without requiring additional parameters to specify NGS asterisms. A real system would in fact ignore the low-order signals from the LGSs, instead using NGS information to provide these corrections. Degradation of AO correction due to tip-tilt indetermination will depend on the NGSs themselves, both location within the field of view and magnitude. We have ignored this consideration here because it is a study in itself (Gilles, Wang & Ellerbroek 2008), and as a consequence, our results are slightly optimistic.

We include both LGS spot elongation and cone effect in these simulations and use a centre of gravity centroiding algorithm to measure local wavefront gradients. We model a sodium layer with a mean 90 km distance from the telescope, with a Gaussian intensity profile with a full width at half-maximum of 10 km. Our simulations contain no NGSs so that we can investigate the tomography purely from the LGSs. We operate in a high-light-level regime, with each sub-aperture receiving 10^6 photons per frame, and photon shot noise is included. The telescope GLAO DM and the individual MOAO DMs have 85 × 85 actuators, unless otherwise stated. In this paper, we concentrate on the on-axis science performance, corresponding to the location furthest from the LGSs, though also present a performance map across the telescope field of view. Unless otherwise stated, results are given for the percentage of ensquared energy within 75 mas in the *H* band (wavelength of 1650 nm), which is a key performance criterion for EAGLE.

We use the GLAO DM to perform a global ground-layer correction across the field of view (since this is conjugated to the telescope pupil). The MOAO DMs are then used to correct only higher layer turbulence, i.e. the MOAO DMs are not used for any ground-layer correction. We make this distinction because the GLAO DM operates in closed loop while the MOAO DMs operate in open loop (i.e. the WFSs are not sensitive to changes on these DMs). The GLAO and MOAO DMs are therefore correcting independent turbulence with no interplay between them, as demonstrated in Fig. 1. In the cases where the MOAO DM is of a lower order than the GLAO DM, we realize that the actuators of these two DMs will not be co-aligned at the ground layer, and thus it might be possible to reduce DM fitting error by using the MOAO DM to remove some of the residual ground-layer turbulence corrected by the GLAO DM. However, we do not do this so as to maintain a clear distinction between the GLAO and MOAO corrected turbulence.

The tomographic wavefront reconstruction is performed at the nine turbulent layers, and the spacing between reconstructed phase

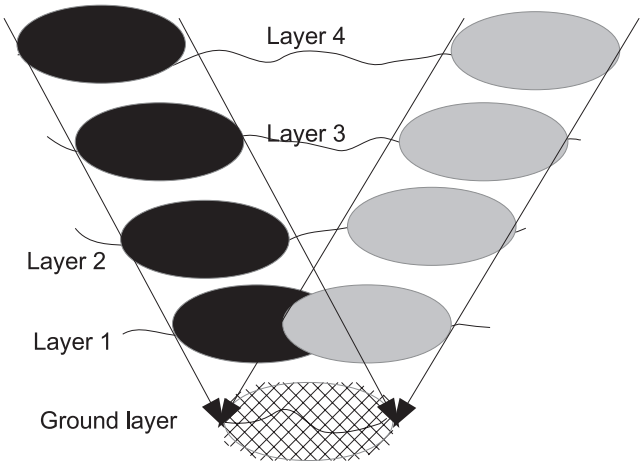

Figure 1. The separation of GLAO and MOAO DM correction. The GLAO DM (hatched) is used to perform a global ground-layer correction, while the MOAO DMs (one performing correction of light grey areas and one performing correction of dark grey areas) only correct higher layers along individual lines of sight and perform no additional ground-layer correction.

Table 1. The atmospheric layer heights above the primary mirror and corresponding layer strengths used in the simulations here, taken from Le Louarn et al. (2012).

C_n^2 profile	Layer 1	Layer 2	Layer 3	Layer 4	Layer 5	Layer 6	Layer 7	Layer 8	Layer 9
Height (m)	47	140	281	562	1125	2250	4500	9000	18 000
C_n^2 (per cent)	52.24	2.6	4.44	11.6	9.89	2.95	5.98	4.3	6
Speed (m s^{-1})	4.55	12.61	12.61	8.73	8.73	14.55	24.25	38.8	20.37
Direction (°)	0	36	72	108	144	180	216	252	288

points is dependent on the relative layer strength and layer height (Gavel et al., private communication) according to

$$N_i = \left[\frac{D_i r_0}{D_0 r_i}\right]^{\frac{10}{11}} N_0, \quad (1)$$

where N_i is the number of phase points in the ith layer with $N_0 = 85$, D_i is the diameter of this layer (which changes with height due to the non-zero field of view) and r_i is Fried's parameter for layer i.

We assume an AO frame rate of 250 Hz and run simulations for 40 s of telescope time (10 000 iterations) to ensure that the science point spread function (PSF) is well averaged, which we verify, and use a non-varying r_0. The chosen frame rate is the baseline for EAGLE, and, although low, the nature of open-loop systems means that AO system bandwidth is higher than an equivalent closed-loop system.

Wavefront reconstruction is performed using a regularized least-squares formulation, based on a sparse Laplacian approximation of the phase covariance (Ellerbroek 2002). Since our light levels are high and slope measurements almost noiseless, this approximates to a minimum variance formulation, though is slightly pessimistic. We assume zero error caused by the reconstruction of pseudo-open-loop slope measurements which would be typical of a DM with closed-loop feedback as is the case with the E-ELT GLAO DM (M4). A fitting step is used to fit the reconstructed volume of turbulence on to the DMs.

2.1 Investigations of LGS asterism radius

It is known that analytical AO modelling codes, for example Fourier domain-based codes, give optimistic performance estimates for wide-field AO systems (Le Louarn et al. 2012), primarily due to the assumption of infinite telescope diameter. The optimum LGS asterism radius for EAGLE and other MOAO systems is subject to some uncertainly, and so here we investigate AO performance as a function of the asterism radius. Our results are also compared with those from an analytical model (a Fourier domain code; Neichel et al. 2008) and with the ESO OCTOPUS simulation code, as given by Le Louarn et al. (2012). The results presented here are also equally applicable to laser tomographic AO systems due to the nature of the tomographic problem.

2.2 Investigations of actuator count

Designs for MOAO instruments such as EAGLE typically specify the science channel DMs to have an actuator pitch equal to the WFS sub-aperture pitch. For EAGLE, this therefore corresponds to a requirement for twenty 85×85 actuator DMs. Current DM technologies have not been scaled to this many actuators, and development of a suitable high-order DM technology will introduce both cost and risk to an ELT MOAO instrument. Here, we investigate the impact that reducing MOAO DM actuator count has on AO performance. We take advantage of a GLAO DM, which has a pitch equal to that of the WFSs, providing a global AO correction. Ground-layer turbulence is often strongest (Osborn et al. 2010), so we hypothesize that once a GLAO correction has been applied, a reduced actuator count might then be sufficient to perform AO correction of the remaining turbulence along the line of sight of each science object without significantly reducing performance. We also investigate the impact on AO performance if the GLAO DM actuator count is also reduced simultaneously with the MOAO DM, for completeness.

To perform these investigations, our simulation consists of a GLAO DM, which is used to correct the tomographically estimated ground-layer turbulence, and an MOAO DM, which corrects the higher layer turbulence along the direction of the science object.

Here, we consider only the case where the MOAO DMs are conjugated to the ground level. However, Basden et al. (2012b) have previously demonstrated the benefit of conjugating MOAO DMs above the ground level, allowing a directional correction to be applied, widening the MOAO field of view by reducing anisoplanatism inside the MOAO field. Because we simulate only a single atmospheric layer at the ground level, our GLAO correction may be optimistic, and a further study of this effect is planned in future work.

2.3 Investigations of mechanical stroke requirements

The DMs used for science channel correction in an MOAO system are likely to have limited stroke, due to a combination of small physical size and high actuator density. A large number of such DMs are required for an MOAO instrument, and so the reduction in cost that can be made by reducing the DM stroke requirement can be significant. We investigate the impact that reducing stroke will have on AO performance by considering two cases. First, the GLAO DM has unlimited stroke, whilst the MOAO DM has a restricted stroke. Secondly, for completeness, we consider the case when all correction is performed by the MOAO DMs, and the impact that limited stroke then has. We simulate a restricted stroke by clipping DM actuators to the maximum allowed mechanical stroke.

2.4 Investigations of DM misalignment

The relative alignment between WFSs and DMs is critical for any AO system, and the tolerance to which the alignment between these components must be maintained is an important design consideration. We investigate the impact that misalignments have on AO system performance, including both lateral shifts and rotations. To model these effects, we shift or rotate the DM surface once the DM demands have been applied to the mirror, and thus the corrected wavefront contains the effects of these shifts and rotations. Here, we do not consider the GLAO and MOAO DMs separately; rather for simplicity, we use only an MOAO DM (also correcting the ground layer), and shift or rotate this.

3 RESULTS AND DISCUSSION

3.1 LGS asterism radius

An AO system with multiple NGSs will always offer best on-axis performance when the asterism radius is zero, i.e. the single conjugate AO case. However, with LGSs, this is not the case. Due to the finite altitude of the LGSs, focal anisoplanatism is observed, thereby reducing AO performance. The effect of focal anisoplanatism can be reduced by using multiple LGSs to sample a greater volume of atmosphere above the telescope. Increasing the radius of the LGS asterism past some optimal diameter will however reduce AO performance due to poor sampling of higher altitude turbulence. Fig. 2 shows simulation results as a function of the asterism radius, comparing our Monte Carlo results with both Monte Carlo results from another independent Monte Carlo code (ESO OCTOPUS; Le Louarn et al. 2012) and an analytic Fourier code (Neichel et al. 2008). These simulations all use parameters as closely matched as possible, including the same atmospheric turbulence profiles, telescope

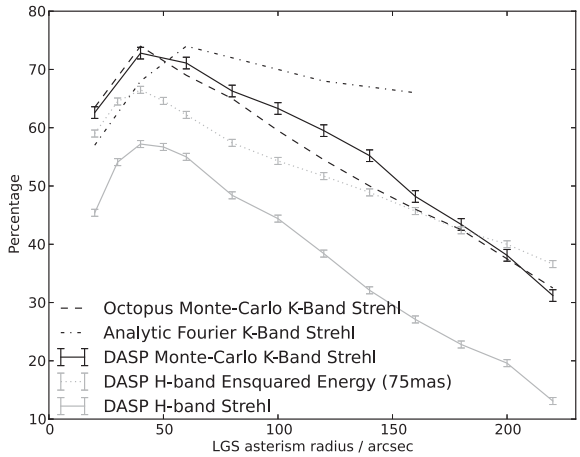

Figure 2. On-axis *K*-band Strehl ratio (black lines) as a function of the LGS asterism radius. The black solid curve presents the DASP results that we have obtained, the dashed curve is from the ESO OCTOPUS Monte Carlo simulation and the dot–dashed is from an analytic Fourier code. For comparison with the remainder of this paper, *H*-band results are also shown in grey, with dotted grey being ensquared energy within 75 mas and solid grey being the Strehl ratio.

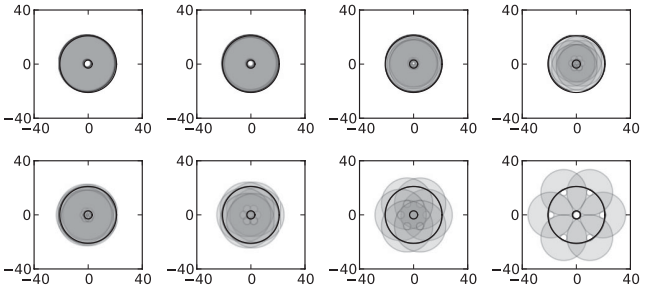

Figure 3. LGS overlap at different atmospheric heights for an asterism radius of 40 arcsec (top row) and an asterism radius of 220 arcsec (bottom row). The LGS beacon is focused at 90 km, and overlap at 2.25, 4.5, 9 and 18 km is shown. The scale is in metres.

diameter, guide star number and DM order. These results are for the *K*-band Strehl ratio (2.2 μm). As can be seen, the Monte Carlo codes are in close agreement. The optimum asterism radius is shown to be about 40 arcsec, and Fig. 3 shows the LGS overlap for different atmospheric heights at this diameter, showing that the on-axis cone of turbulence is indeed well sampled except for at the edges of the very highest layer. The overlap for the nominal EAGLE asterism radius of 220 arcsec is also shown, displaying reduced guide star overlap, corresponding to poorer reconstruction of turbulence, particularly at higher altitudes. It should be noted that the analytic code gives a different slope for the dependency of performance on the asterism radius, due to the infinite pupil assumption (Le Louarn et al. 2012).

Fig. 4(a) shows *H*-band ensquared energy within 75 × 75 mas over the entire EAGLE field of view, with a 220 arcsec LGS asterism radius. Over the 5 arcmin science field (represented by a grey circle), the variation in ensquared energy ranges from 35 to 40 per cent. Fig. 4(b) shows the variation of the Strehl ratio over this field. Taking advantage of NGSs available within the technical field of view would allow this performance to be increased (Rousset et al. 2010) though we do not consider this further here.

Throughout the rest of this paper, results are given for *H*-band ensquared energy within 75 mas, and for comparison purposes, these results are also shown in Fig. 2. The error bars in this figure are

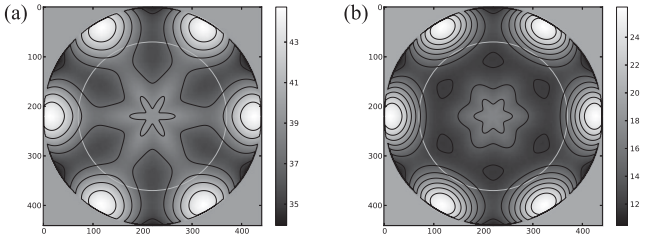

Figure 4. (a) *H*-band MOAO performance (ensquared energy in 75 × 75 mas) over the 440 arcsec technical field of view of an EAGLE-like instrument, with an LGS asterism diameter of 440 arcsec. The centred grey circle represents a 5 arcmin field, and contours are spaced by 2 per cent, starting at 35 per cent ensquared *H*-band energy. (b) As for (a), showing the Strehl ratio over the field.

calculated from the variance of multiple simulation runs, and are at the sub 1 per cent level for all further results presented here, and thus are not shown for clarity.

3.2 Actuator count

It can be seen from Fig. 5 that when a GLAO DM is present, the actuator density for MOAO DMs (which perform only higher layer correction) can be relaxed somewhat without dramatically affecting AO performance. This is an encouraging result for MOAO system designers, because it allows what is a high-cost single component (the DM), of which many (20 for EAGLE) are required for an MOAO system, to have its specification reduced. Additionally, this reduces the computational demands (which typically scale as the square of the total number of actuators) placed on the necessary real-time control system (Basden et al. 2010b) (nearly a factor of 3 reduction in computational requirements moving from 85 × 85 to 65 actuators). For EAGLE this is important, because although it has been shown that real-time control on this scale is a tractable problem (Basden & Myers 2012), reducing computational demands in wavefront reconstruction will provide the opportunity for additional algorithms to be used to further improve AO system performance,

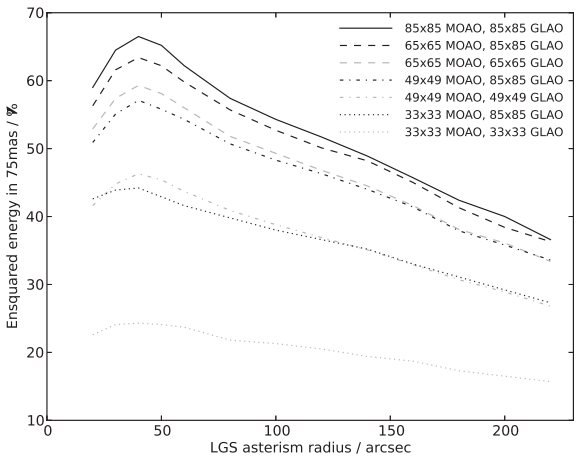

Figure 5. AO performance as a function of the LGS asterism radius for the different DM actuator counts given in the legend. A ground-layer (GLAO) correction followed by an MOAO correction (with no ground-layer component) is performed. Stroke is unlimited for both DMs. It should be noted that cases with equal order for both GLAO and MOAO DMs are identical to a case using only an MOAO DM of the same order that includes ground-layer correction and is not stroke limited.

such as the brightest pixel selection algorithm (Basden, Myers & Gendron 2012a) successfully demonstrated with CANARY.

The presence of a high-order GLAO DM is, unsurprisingly, helpful, compared with the case where both DMs are of equal, lower, order (which is identical to using only an MOAO DM of this order, also including ground-layer correction, in these simulations). This is because using a higher order GLAO DM reduces the fitting error of the DM to ground-layer turbulence (which increases with actuator pitch). In particular, if the MOAO DM order is dropped to 33 × 33 actuators, which represents a readily available DM, AO performance is doubled when the GLAO DM is present at full 85 × 85 actuators (E-ELT M4 scale) compared to when this is also dropped to 33 × 33 actuators (which is also equivalent to not using a GLAO DM, and using the MOAO DM to perform all correction including the ground layer). We can see from Fig. 5 that there is only a small performance loss of about 2–3 per cent when using a 65 × 65 actuator MOAO DM compared with a 85 × 85 actuator DM when the GLAO DM is present. It should be noted that we have used these DM actuator counts for ease of simulation, and that removing one row and column to match currently available DMs (for example, the 64 × 64 and 32 × 32 actuator DMs available from Boston Micromachines) will have little impact on performance, as can be seen from the trend of performance with actuator count.

3.2.1 Pseudo-open-loop control considerations

Changes applied to the GLAO DM on the E-ELT are sensed by the WFSs, and thus it is necessary to operate using a pseudo-open-loop controller so that minimum variance wavefront reconstruction can be performed. There will always be some uncertainty in the mirror surface shape, however small, and this will lead to a non-zero pseudo-open-loop error, though this will be minimized by accurate DM surface position sensors (either optical or mechanical). It is interesting to consider the impact of this error source here.

If the MOAO DM actuator count is to be constrained for cost reasons, we have the choice of either using it alone or in conjunction with the higher order GLAO DM accepting the additional pseudo-open-loop error. DM fitting error in radians squared is given approximately by (Hardy 1998, p. 196)

$$\sigma_{\mathrm{F}}^2 \approx f \left(\frac{d}{r_0} \right)^{\left(\frac{5}{3}\right)}, \tag{2}$$

where f is a constant that depends on the DM (typically around 0.28), d is the actuator pitch and r_0 is Fried's parameter.

Considering only the effect of ground-layer turbulence, at 1650 nm, this gives a fitting error contribution of about 57 nm for an 85 × 85 actuator DM, 71 nm for a 65 × 65 actuator DM, 91 nm for a 49 × 49 actuator DM and 127 nm for a 33 × 33 actuator DM. Therefore, if we perform ground-layer correction with a closed-loop 85 × 85 actuator DM, we can accept up to 42 nm pseudo-open-loop error, and still obtain better performance than if using an open-loop 65 × 65 actuator DM (by adding error terms in quadrature). Likewise, we can accept up to 71 nm pseudo-open-loop error before it is better to use a 49 × 49 actuator open-loop DM and up to 113 nm error before it is better to use a 33 × 33 actuator open-loop DM. The actual pseudo-open-loop error for the E-ELT M4 DM is not yet known; however, one would hope that it would be below these levels due to accurate position sensors.

3.3 DM stroke requirements

The E-ELT contains a large DM as part of the telescope optical train conjugated close to the ground. This DM is physically large and is expected to have large (essentially unlimited) stoke. The MOAO DMs, of which a large number is required, are likely to have limited stroke, being physically small. Fig. 6 shows the impact of maximum MOAO DM mechanical stroke on AO performance for the case of the narrowest asterism considered here (20 arcsec radius). In this case, the GLAO DM is assumed not to be stoke limited. Fig. 7 shows AO performance as a function of the LGS asterism radius for the case of unlimited MOAO DM stroke, and with stroke limited to 1.5 and 2.5 μm. It is also interesting to see how performance is affected when total stroke is limited, and this is shown in Figs 6 and 7 as a function of the asterism radius. It should be noted that in this case, we assume only one DM, rather than two DMs each with limited stroke, i.e. operation without the GLAO DM.

From Fig. 6, we can see that a maximum mechanical stroke of 3.5 μm for the MOAO DMs will reduce performance by only a fraction of a percentage point when compared with a stroke-unlimited DM. A maximum stoke of 2.5 μm will lead to a slight

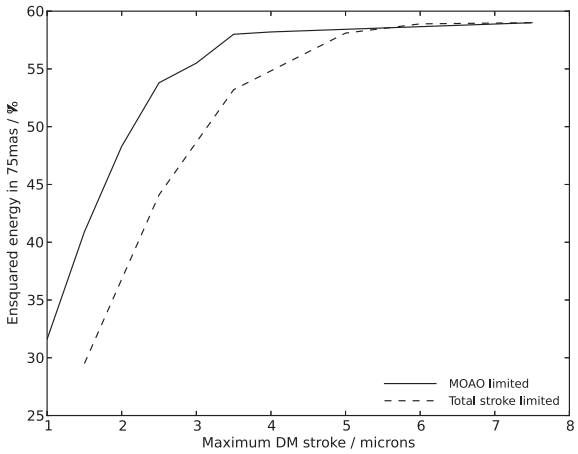

Figure 6. AO performance as a function of the maximum MOAO DM stroke (solid) for an LGS asterism with 20 arcsec radius. Also shown (dashed) is performance when total stroke is limited (i.e. assuming that the GLAO correction is not present).

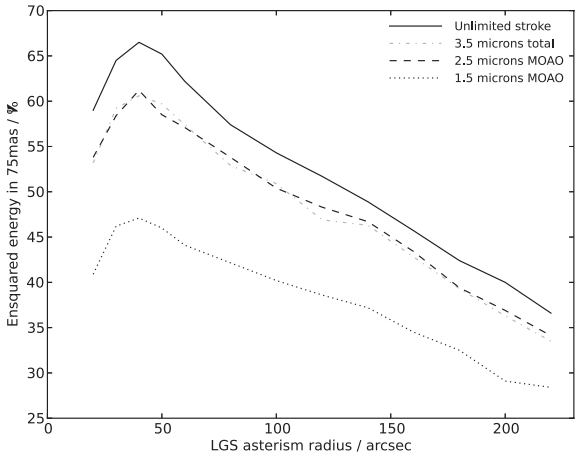

Figure 7. AO performance as a function of the LGS asterism radius, for an MOAO DM with unlimited stroke (solid), a maximum stroke of 2.5 μm (dashed) and a maximum stroke of 1.5 μm (dotted).

reduction in performance, while limiting stroke to 1.5 μm reduces performance by a third. It is interesting to note that the presence of the GLAO DM allows the stroke requirements on the MOAO DMs to be relaxed by about 1 μm (Fig. 6).

3.4 DM misalignments

During AO system calibration, the relative alignment of the WFSs to the DM actuators is generally encoded within the system using a control matrix or other means. Any unobserved deviation in position between the WFSs and DM after the calibration procedure can result in a reduction in system performance.

The rotation of a DM relative to the expected position (and thus the position for which DM demands are computed) affects performance as shown in Fig. 8. It is clear here that performance is affected even for small rotation angles, falling steeply for angles larger than 0.2. This angle corresponds to a shift of about 14 per cent of a sub-aperture for the outer ring of sub-apertures, which is a 2.3 pixel shift in actuator position relative to the WFS sub-aperture. Fig. 9 shows AO performance as a function of the asterism radius when the relative DM rotation is 0.5, with unrotated performance shown for comparison, showing an effectively constant drop in performance when misalignment occurs.

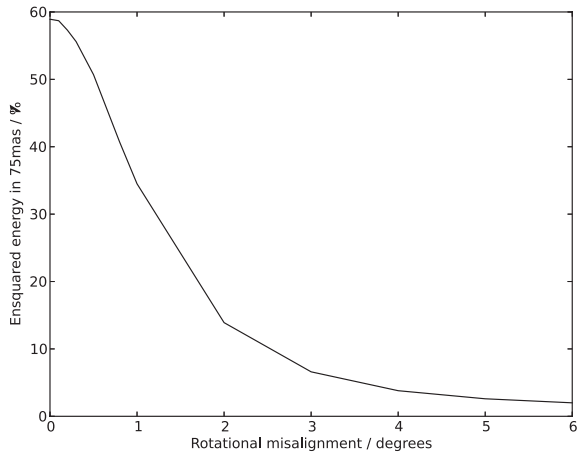

Figure 8. AO performance as a function of the rotational DM misalignment for a 20 arcsec LGS asterism radius (without the GLAO DM).

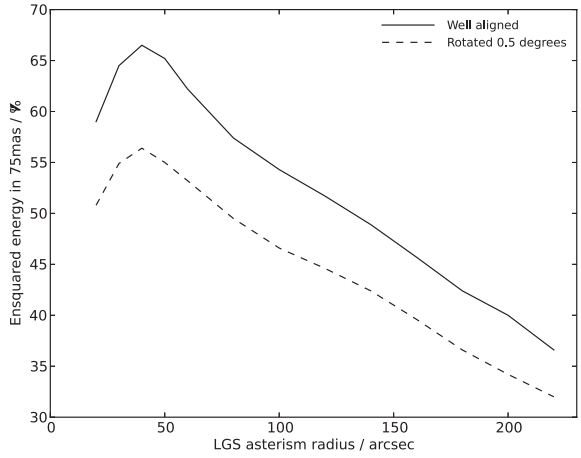

Figure 9. AO performance as a function of the LGS asterism radius for rotational DM misalignments of 0° (i.e. well aligned) and 0.5.

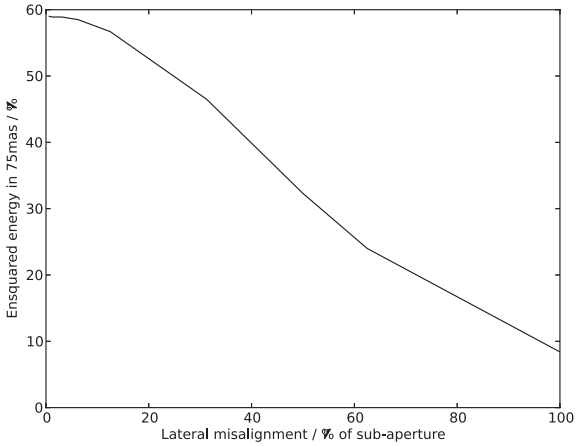

Figure 10. AO performance as a function of the lateral DM misalignment as a percentage of a sub-aperture (with 16 × 16 pixels per sub-aperture), for a 20 arcsec LGS asterism radius.

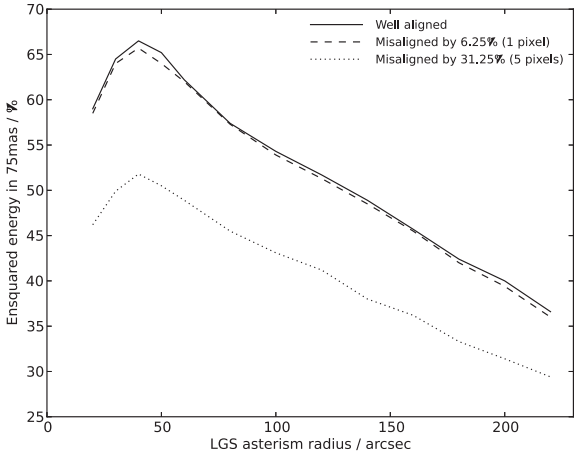

Figure 11. AO performance as a function of the LGS asterism radius for lateral DM misalignments of 0 (i.e. well aligned), 1 and 5 pixels.

The relative lateral shift of a DM between its assumed and actual position affects performance as shown in Fig. 10. Here, we can see that shifts of up to 2 pixels (12.5 per cent of a sub-aperture) lead to only small drops in performance, while for larger misalignments, AO performance begins to fall more rapidly. Fig. 11 shows AO performance as a function of the asterism radius for misalignments of 1 and 5 pixels, as well as the well-aligned case for comparison.

4 CONCLUSIONS

We have investigated the impact of the LGS asterism radius and various DM characteristics, including DM order, maximum mechanical DM stroke and DM alignment tolerances for an ELT-scale MOAO system, using a full end-to-end Monte Carlo AO simulation tool. These simulations have been based on the conceptual designs for the EAGLE MOAO instrument.

We have not sought to give definitive answers to the questions investigated here, rather specifying how AO performance is affected by these parameters. This information can then be used during the design and specification of the relevant instrument. For

example, we have shown that small misalignments of the DM lead to only small drops in AO performance. The performance trade-off decisions that can be made are left to science instrument considerations. However, from our study, it is helpful to make some observations as follows.

AO performance as a function of the LGS guide star asterism radius has been shown to fall more steeply than suggested by Fourier-based analytical codes which assume infinite pupil diameters, confirming previous results (Le Louarn et al. 2012). However, we have shown that for a perfect MOAO system on a 42 m ELT, with six LGSs placed in a ring with an asterism radius of 220 arcsec and with perfect tip-tilt anisoplanatism correction, *H*-band performance across the science field of view is sufficient to give more than 35 per cent ensquared energy within 75 mas of the resulting science PSF, which is better than the requirement for the EAGLE MOAO ELT instrument.

We have shown that the presence of a high-order global GLAO DM allows the requirements for MOAO DMs to be reduced. A 49×49 actuator DM meets the EAGLE on-axis AO performance requirement with the largest LGS asterism radius, if the assumptions made here are valid (namely no misalignment and perfect tip-tilt correction). This will allow the cost of EAGLE to be greatly reduced. Using a 65×65 actuator DM gives almost no reduction in AO performance compared with a full 85×85 actuator DM matched to the WFS sub-aperture count.

To preserve AO performance, the MOAO DMs must have a maximum stroke capability of at least 2.5 μm, with 3.5 μm being a goal.

DM-to-WFS alignment tolerances must be kept to within an eighth of a sub-aperture of calibrated position, so that performance is not significantly affected. For rotation, this represents an angle of 0.°2 being the maximum misalignment from expected DM position to avoid significant performance reductions.

In this study, the effect of NGSs has not been included, meaning that these results are slightly pessimistic, and neither have variations in sodium layer, or telescope vibrations. These issues will be the subject of future work.

ACKNOWLEDGEMENTS

The authors would like to thank M. Le Louarn and G. Rousset for providing advice and comments, and the referees who helped to improve this paper.

REFERENCES

Babcock H. W., 1953, PASP, 65, 229
Basden A. G., 2007, Appl. Opt., 46, 900
Basden A. G., Myers R. M., 2012, MNRAS, 424, 1483
Basden A. G., Assémat F., Butterley T., Geng D., Saunter C. D., Wilson R. W., 2005, MNRAS, 364, 1413
Basden A. G., Butterley T., Myers R. M., Wilson R. W., 2007, Appl. Opt., 46, 1089
Basden A., Myers R., Butterley T., 2010a, Appl. Opt., 49, G1
Basden A., Geng D., Myers R., Younger E., 2010b, Appl. Opt., 49, 6354
Basden A. G., Myers R. M., Gendron E., 2012a, MNRAS, 419, 1628
Basden A., Bharmal N. A., Butterley T., Dipper N., Morris T., Myers R., Reeves A., 2012b, in Ellerbroek B. L., Marchetti E., Véran J.-P., eds, Proc. SPIE Conf. Ser. Vol. 8447, A Study of MOAO behind GLAO for EAGLE. SPIE, Bellingham, p. 84475E
Cuby J.-G. et al., 2008, in McLean I. S., Casali M. M., eds, Proc. SPIE Conf. Ser. Vol. 7014, Ground-Based and Airborne Instrumentation for Astronomy II. SPIE, Bellingham, p. 70141K
Ellerbroek B. L., 2002, J. Opt. Soc. Am. A 19, 1803
Fusco T. et al., 2008, in Hubin N., Max C. E., Wizinowich P. L., eds, Proc. SPIE Conf. Ser. Vol. 7015, Adaptive Optics Systems. SPIE, Bellingham, p. 70150T
Gendron E., Vidal F., Brangier M., Morris T., Hubert Z., Basden A., Rousset G., Myers R., 2011, A&A, 529, L2
Gilles L., Wang L., Ellerbroek B., 2008, in Hubin N., Max C. E., Wizinowich P. L., eds, Proc. SPIE Conf. Ser. Vol. 7015, Adaptive Optics Systems. SPIE, Bellingham, p. 701520
Hardy J., 1998, Oxford Series in Optical and Imaging Sciences: Adaptive Optics for Astronomical Telescopes. Oxford Univ. Press, Oxford
Le Louarn M., Clare R., Béchet C., Talon M., 2012, in Ellerbroek B. L., Marchetti E., Véran J.-P., eds, Proc. SPIE Conf. Ser. Vol. 8447, Simulations of Adaptive Optics Systems for the E-ELT. SPIE, Bellingham, p. 84475D
Neichel B., Fusco T., Conan J.-M., 2008, J. Opt. Soc. Am. A, 26, 219
Nelson J., Sanders G. H., 2008, in Stepp L. M., Gilmozzi R., eds, Proc. SPIE Conf. Ser. Vol. 7012, Ground-Based and Airborne Telescopes II. SPIE, Bellingham, p. 70121A
Osborn J., Wilson R., Butterley T., Shepherd H., Sarazin M., 2010, MNRAS, 406, 1405
Rousset G. et al., 2010, in Ellerbroek B. L., Hart M., Hubin N., Wizinowich P. L., eds, Proc. SPIE Conf. Ser. Vol. 7736, Adaptive Optics Systems II. SPIE, Bellingham, p. 77360S
Spyromilio J., Comerón F., D'Odorico S., Kissler-Patig M., Gilmozzi R., 2008, The Messenger, 133, 2

This paper has been typeset from a TEX/LATEX file prepared by the author.